Title
Heat of Mixing During Fast Charge/Discharge of a Li-Ion Cell: A Study on NMC523 Cathode

Journal
Journal of The Electrochemical Society, 167(9)

ISSN
0013-4651

Authors
Chalise, Divya
Lu, Wenquan
Srinivasan, Venkat
et al.

Publication Date
2020-01-07

DOI
10.1149/1945-7111/abaf71

Peer reviewed

Heat of Mixing During Fast Charge/Discharge of a Li-Ion Cell: A Study on NMC523 Cathode

Journal of The Electrochemical Society, 2020 **167** 090560

Heat of Mixing During Fast Charge/Discharge of a Li-Ion Cell: A Study on NMC523 Cathode

Divya Chalise,[1,2] Wenquan Lu,[3] Venkat Srinivasan,[3,z] and Ravi Prasher[1,2,z]

[1]*Department of Mechanical Engineering, University of California, Berkeley, California, 94720, United States of America*
[2]*Energy Technologies Area, Lawrence Berkeley National Lab, 1 Cyclotron Road, Berkeley, California 94720, United States of America*
[3]*Argonne National Laboratory, Lemont, Illinois 60439, United States of America*

Predicting temperature rise accurately during fast charge/discharge of a Li-ion cell is essential to avoid thermal runaway and extend battery life. While modeling the temperature rise, it is necessary to model the heat generation correctly. Heat of mixing, one of the four main sources of heat generation in a Li-ion battery, has often been considered insignificant and therefore excluded from modeling. When included, it is modeled using the expression from a Taylor expansion approximation. In this work, we have shown the conditions when including the heat of mixing becomes important and quantified the error associated with using the Taylor expansion, especially under high charge/discharge conditions. Consequently, we carry out the calculation of the rate of enthalpy change and the heat generation rate from the most fundamental equation for the rate of the total enthalpy change without simplifying assumptions or approximations. The heat generation rate calculated doing so naturally includes irreversible, reversible and mixing heat. We then exclusively separate out the heat of mixing by subtracting the rate of enthalpy change by reaction from the rate of the total enthalpy change. Results show that the contribution of heat of mixing in the total heat generated increases with the charge/discharge rate and is as large as 23% for a 6 C discharge. This result suggests that while modeling heat generation for fast charge/discharge, it is necessary to include the heat of mixing and avoid calculating it using the Taylor expansion approximation.

 [DOI: 10.1149/1945-7111/abaf71]

Manuscript submitted March 30, 2020; revised manuscript received July 21, 2020. Published August 26, 2020. *This paper is part of the JES Focus Issue on Battery Safety, Reliability and Mitigation.*

List of symbols

U	Open Circuit Potential (V)
V_{cell}	Terminal Voltage (V)
$V_{surface}$	Potential difference between the surface of the solid phase and the electrolyte (V)
T	Temperature (K)
c	Concentration (mol m^{-3})
y	Lithium Stoichiometry in the insertion compound
t	Time (s)
H	Enthalpy (J)
$\bar{H}$	Partial Molar Enthalpy (J mol^{-1})
F	Faraday's Constant (C mol^{-1})
r	Radial position (m)
x	Position in electrode (m)
$\bar{V}$	Molar Volume of a Insertion compound (m^3 mol^{-1})
v	Volume (m^3)
I	Applied Current Density (A m^{-2})
i	Current Density seen by a particle (A m^{-2})
I_p	Total Current experienced by a particle (A)
j	Reaction Current (A m^{-3})
$\dot{Q}$	Heat generated (W m^{-2})
$L_{cathode}$	Thickness of Cathode (m)
$L_{separator}$	Thickness of Separator (m)
ε_{ins}	Volume Fraction of Active material in cathode
ε_f	Volume fraction of inactive material in cathode
ε_{sep}	Volume fraction of polymer in the separator
R	Radius of active material particle (m)
k_0	Reaction rate constant for cathode (mol s^{-1})
α_a	Anodic Charge transfer coefficient
α_c	Cathodic charge transfer coefficient
R_{SEI}	Electrical Resistance of SEI Layer
$\sigma_{cathode}$	Bulk Conductivity of Cathode (S m^{-1})
$c_{e,i}$	Initial electrolyte concentration (M)
c_e	Electrolyte concentration (M)
t_+	Transfer Coefficient
p	Bruggeman Porosity Exponent
κ	Ionic Conductivity of electrolyte (S m^{-1})
D_e	Li-ion diffusion coefficient in electrolyte (m^2 s^{-1})
D_s	Solid Li Diffusion coefficient in active material (m^2 s^{-1})

Subscripts

m	Matrix
s	Active Material (solid)

Understanding temperature rise is a critical aspect of enabling battery fast charging.[1–3] High temperature accelerates ageing[1,4] and triggers thermal runaway reaction.[1,5,6] In order to predict temperature rise, it is essential to understand how the heat generation evolves with time during a charge or a discharge process. It is well agreed upon in literature that the four main sources of heat generation in a battery are irreversible heat (Ohmic and kinetic losses), reversible (entropic) heat, heat due to side reactions and heat of mixing.[7–14]

Various models in literature for predicting heat generation in batteries can broadly be divided into two classes: models assuming uniform current distribution and models using non-uniform current distribution. The simplest uniform current models for time dependent heat generation in a galvanostatic (constant current) charge or discharge of a cell include a time or average State-Of-Charge (SOC) dependent voltage (V_{cell}), Open Circuit Potential (U) and entropic (dU/dT) terms to account for heat released due to irreversible Ohmic and kinetic losses as well as entropic changes.[13,15–18] As U, V and dU/dT change with time (or SOC), these models predict a total heat generation that evolves with time. However, an implicit assumption in these models is that there is no mass transport limitation. It is assumed that all the active material particles in a particular electrode are at the same state of charge and there is no concentration variation within the particles themselves. Some models[19–22] try to include the effect of concentration gradients by including an additional heat of mixing term. However, the heat of mixing term is generally computed using an expression obtained by Taylor expansion, which, as discussed later in the paper, is not applicable at high currents where concentration gradients are significant.

[z]E-mail: vsrinivasan@anl.gov; rsprasher@lbl.gov

The non-uniform current distribution models are rigorous in accounting for spatial inhomogeneity in heat generation caused by mass transport limitations and current non-uniformity. Generally, these models obtain the current distribution by solving Newman's Pseudo-2D (P2D) model and incorporate a spatially and temporally varying heat generation expression.[23–26] The heat generation term includes irreversible heat arising from losses in transport within the electrolyte, the electrodes and the current collectors and reaction heat arising from surface overpotential. Additionally, these models account for entropic change due to the reaction at the surface of an active material particle. However, they do not account for heat of mixing i.e. enthalpy change due to temporally and spatially varying composition within an active material particle. After a charge transfer reaction, the solid lithium diffuses in an intercalation compound. The composition of the intercalation compound determines its energy,[7] and as the composition changes when the lithium diffuses in the active material particle, the energy of the active material particle changes with time. This change in the energy is manifested as heat and is generally known as the heat of mixing in the particles.

Some of the earliest and the most fundamental work in quantifying heat of mixing in batteries were carried out by Thomas and Newman,[7,9,14] where they describe heat of mixing as the enthalpy change due to the formation or relaxation of concentration gradients. Their work presents an approximate expression to estimate the magnitude of heat of mixing (Eq. 40 in Ref. 7) derived using Taylor expansion of the composition dependence of enthalpy. The Taylor expansion implicitly assumes small changes in the composition and therefore cannot be applied in cases where concentration gradients are significant. Since heat of mixing itself is insignificant in the absence of strong concentration gradients, this approach of Taylor expansion is not particularly useful. However, various authors[19–21,27,28] have used the same expression (Eq. 40 in Thomas and Newman[7]) to include the effect of mixing in their study of heat generation. It will be shown later in the paper that at high charge/discharge rates, this approach can give misleading results and should be avoided when mass transport effects become significantly important. Thomas et al.[7] have also provided expressions to estimate the heat released or consumed (Eq. 46 in Ref. 7) when the concentration gradients relax after the current is switched-off. In doing so, they have used the pseudo-steady state assumption to solve for the concentration profile. This assumption is valid when the temporal variation of the concentration is much smaller compared to the spatial variation. This can be true when the battery has already operated for a significant amount of time. Therefore, this is a reasonable approach to obtain the concentration profile at the time when the current is switched-off (as in the case modeled by Thomas et al.[7]). However, these equations are not valid when the concentration profile is still evolving with time, and therefore the time derivative of the enthalpy of relaxation given by these equations cannot be used to model heat of mixing during operation of the cell. Still, it is seen in some of the previous works[27] that authors have used the time derivative of enthalpy of relaxation to calculate the heat of mixing for the entire duration of operation of a cell. From the review of the past literature, it is therefore evident that there is a need to illustrate the limitations of Thomas' method based on Taylor expansion and to prescribe a suitable method for calculating the heat of mixing in fast charge/discharge conditions.

In this paper, we carry out the calculation of the rate of total enthalpy change for the active material particles in a cell and separate it from the total work done by the cell to obtain a heat generation term that naturally includes heat of mixing along with other reversible and irreversible heat terms. Finally, we separate out the irreversible and reversible reaction heat to come up with an explicit term for heat of mixing in an active material particle. In doing so, we avoid assumptions such as the applicability of pseudo steady state or the existence small concentration gradients. Avoiding the pseudo-steady state assumption makes the method applicable to studying heat of mixing at any time of operation of the cell, and avoiding the small concentration gradient assumption makes it suitable in studying heat of mixing during fast charging.

Theory: Rate of Total Enthalpy Change

We begin by investigating the rate of total enthalpy change in a single particle and extend it to the entire cell.

For a lithium insertion electrode, we can assume a spherical active material particle and assume it to comprise of a matrix (m) and inserted solid lithium (s). Then, the total enthalpy of the particle is given by the sum of enthalpies of the matrix and the lithium. Since the concentration of Li can be a function of space, we need to formulate a volumetric integral of concentration and the enthalpy of each species associated with that concentration to calculate the total enthalpy:

$$H = \int (c_s \overline{H_s} + c_m \overline{H_m}) dv \qquad [1]$$

where, c_s and c_m are the concentration of lithium and the matrix respectively, $\overline{H_s}$ and $\overline{H_m}$ are the respective partial molar enthalpies of lithium and the matrix in the cathode or anode compound, and the integral is over the volume of the particle.

Then, the rate of change of enthalpy is given by:

$$\frac{dH}{dt} = \int \left(\left(\frac{dc_s}{dt} \right) \overline{H_s} + \left(\frac{dc_m}{dt} \right) \overline{H_m} + \left(\frac{d\overline{H_s}}{dt} \right) c_s + \left(\frac{d\overline{H_m}}{dt} \right) c_m \right) dv \qquad [2]$$

From Gibbs-Duhem Relation, it can be shown that

$$\left(\frac{d\overline{H_s}}{dt} \right) c_s + \left(\frac{d\overline{H_m}}{dt} \right) c_m = 0 \qquad [3]$$

Then,

$$\frac{dH}{dt} = \int \left(\left(\frac{dc_s}{dt} \right) \overline{H_s} + \left(\frac{dc_m}{dt} \right) \overline{H_m} \right) dv \qquad [4]$$

Since the concentration of the matrix does not change with time, $\left(\frac{dc_m}{dt} \right) = 0$.

Additionally, Newman has shown that $\overline{H_s} = -FU_H$.[7,8] Here, F is the Faraday's constant and U_H is the enthalpic potential defined by:

$$U_H = U - T \frac{\partial U}{\partial T} \qquad [5]$$

Therefore, the expression for the total enthalpy change becomes:

$$\frac{dH}{dt} = -F \int \left(\left(\frac{dc_s}{dt} \right) U_H \right) dv \qquad [6]$$

For a spherical particle, the volumetric integral becomes:

$$\frac{dH}{dt} = -4\pi F \int_0^R r^2 \left(\frac{dc_s(r,\, t)}{dt} \right) U_H(y(r,\, t)) dr \qquad [7]$$

Equation 6 (or equivalently Eq. 7 for a spherical particle) is the most fundamental equation to calculate the enthalpy change for a Li-insertion compound at constant temperature. This equation was presented by Bernardi and Newman (1985) (Eq. 5 in Ref. 16) and has been used and further simplified by various authors to calculate the enthalpy change and heat generation (e.g., Eq. 8 in Rao and Newman (1997),[13] Eq. 11 in Thomas and Newman (2003)[7]). In fact, as shown by Rao and Newman,[13] the most commonly used expression for the rate of enthalpy change i.e. *Rate of Enthalpy Change* $= IU_H = IU - IT\frac{\partial U}{\partial T}$ is a simplification of Eq. 6. Similarly, as discussed later, the Taylor expansion formulation[7] is also a simplification of Eq. 6.

Table I. Parameters used in P2D Simulation.

Parameter	Value
$L_{cathode}$	42 μm[a)]
$L_{separator}$	25 μm[a)]
ε_{ins}	0.716[a)]
ε_f	0.083[a)]
ε_{sep}	0.41[a)]
R	6 μm[a)]
k_0	1×10^{-11} mol s^{-1}[39]
α_a	0.5[33]
α_c	0.5[33]
R_{SEI}	0[33]
$\sigma_{cathode}$	10 S m^{-1}[33]
$c_{e,i}$	1.2 M[33]
t_+	0.363[33]
p	1.5[33]
κ	$15.8 \times 10^{-1} c_e \exp\left(-13472\left(\frac{c_e}{1000}\right)^{1.4}\right)$[33]
D_e	4×10^{-10} m^2 s^{-1}[40]
D_s	3×10^{-14} m^2 s^{-1}[41]
t_+	0.363[33]

a) = standard value for the coin cell provided by CAMP.

From Eq. 7, in order to calculate the total enthalpy change, we need to determine the time evolution of the concentration of lithium as a function of space (r). If the local concentration of lithium is known, the local state of charge ($y(r, t)$) can be determined from:

$$c\,(r,\,t)\;=\;\frac{y\,(r,\,t)}{\bar{V}} \qquad [8]$$

It is to be noted that Eq. 8 assumes negligible volume change in the particle with the insetion/deinsertion of lithium, which is a reasonable assumption for most electrode materials.[29–31]

To obtain the concentration profile, the diffusion equation (Eq. 9) for the particle needs to be solved.

$$\frac{\partial c}{\partial t}\;=\;D_s\frac{1}{r^2}\frac{\partial}{\partial r}\left(r^2\frac{\partial c}{\partial r}\right) \qquad [9]$$

Where, D_s is the diffusivity of lithium in the insertion compound.

The required boundary conditions are:

$$\text{Symmetry: } \frac{dc}{dr}\;=\;0 \text{ at } r\;=\;0$$
$$\text{Faraday's Law: } D_s\left(\frac{dc}{dr}\right)\;=\;-\frac{i}{F} \text{ at } r\;=\;R \qquad [10]$$

with the initial condition:

$$c(r,\,0)\;=\;c_0(r) \qquad [11]$$

where, $c_0(r)$ is the concentration profile obtained at the end of the previous time iteration in the simulation of the concentration profile.

The current density (i) experienced by each particle can be obtained from[8]:

$$i(x)\;=\;\frac{R}{3\varepsilon_{ins}}\left(\frac{dI}{dx}\right)\;=\;\frac{R}{3\varepsilon_{ins}}j(x) \qquad [12]$$

The reaction current ($j(x)$) can be obtained by solving the P2D model.[32,33]

Solving Eq. 9 allows us to compute the volumetric integral given by Eq. 7 to calculate the total enthalpy change for a particle.

The total enthalpy change for the entire cell is the sum of enthalpy change for all the particles in both electrodes. Since the total heat generated in a discharge process is the difference between the total enthalpy change and the useful work produced (IV), we can therefore write the expression for the total heat generated as:

$$\textit{Total Heat Generated } (Q)\;=\;\sum_{\textit{Electrodes}}\;\sum_{\textit{Particles per unit area}}\left(\frac{dH}{dt}\right)\;-\;IV_{cell} \qquad [13]$$

Equation 13 implicitly includes heat generation from all mechanisms including transport and kinetic losses and heat of mixing within the particles. Therefore, Eq. 13 is the most general equation to calculate the total heat generated.

If we have to isolate the heat of mixing in a particle itself, we would have to consider the total heat generated in the particle and separate the irreversible and reversible heat generated due to the reaction on the surface.

Following the same logic as in Eq. 13, the total heat generated by a particle is:

$$\dot{Q}_{Total,\,particle}\;=\;\left(\frac{dH}{dt}\right)\;-\;4\pi R^2 iV_{surface} \qquad [14]$$

Here, $V_{surface}$ is the potential difference between the surface of the solid phase and the electrolyte.

The reversible and irreversible heat of reaction for the particle is obtained from[25]:

$$\dot{Q}_{reaction,particle}\;=\;4\pi R^2(iU_{H,surface}\;-\;iV_{surface}) \qquad [15]$$

Since the expression for the total heat generated includes heat of mixing and the heat of reaction, the explicit expression for heat of mixing in a particle is:

$$\dot{Q}_{mixing,particle}\;=\;Q_{Total,particle}\;-\;Q_{reaction,particle} \qquad [16]$$

$$\dot{Q}_{mixing,particle}\;=\;\left(\frac{dH}{dt}\right)\;-\;4\pi R^2 iU_{H,surface} \qquad [17]$$

For the entire cell,

$$\dot{Q}_{mixing,Cell}\;=\;\sum_{\textit{Electrodes}}\;\sum_{\textit{Particles per unit area}}\left(\left(\frac{dH}{dt}\right)\;-\;4\pi R^2 iU_{H,surface}\right) \qquad [18]$$

Therefore, in a mathematical sense, the heat of mixing is equivalent to the error induced in calculating the heat generation by only considering the enthalpy change of the reaction at the surface instead of the total enthalpy change of the particle.

Simulation Details

This study is carried out for a Li-ion cell with NMC523 ($Li_xNi_{0.5}Co_{0.3}Mn_{0.2}O_2$) cathode and Li-metal anode with $LiPF_6$ electrolyte in EC:DMC solvent. In order to quantify the enthalpy change using Eq. 6, it is necessary to quantify the enthalpy potential (U_H) as a function of the state of charge. It has two components: Open-Circuit potential (U) and the entropic coefficient (dU/dT). These quantities were measured for a coin-cell with NMC523 cathode and Li-metal anode obtained from the Cell Analysis, Modeling, and Prototyping (CAMP) Facility at Argonne National Laboratory. The Open Circuit Potential for NMC523 was obtained by measuring the cell voltage (V_{cell}) as a function of the state of charge for a very slow discharge (C/10) assuming the losses to be negligible so that the cell voltage would be equal to the Open-Circuit potential. The entropic coefficient (dU/dT) was determined from

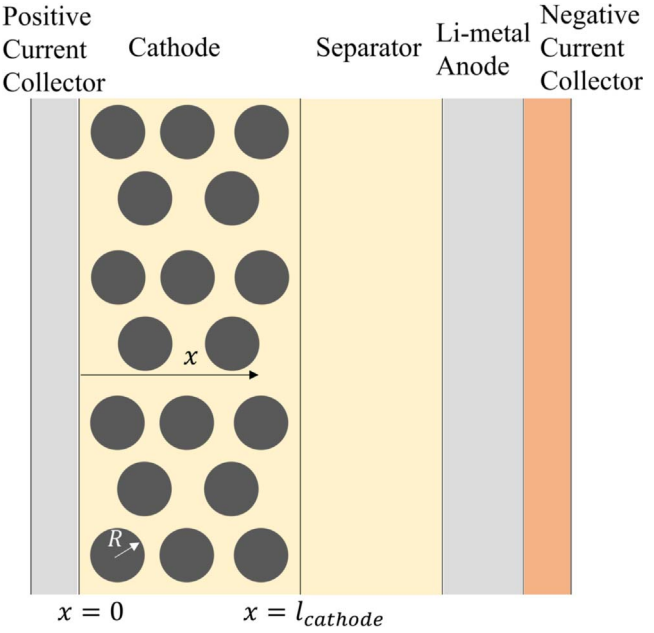

Figure 1. Schematic of the Simulation setup.

calorimetry using the method described in the literature.[14,34–36] The measured data for the Open Circuit Potential and the entropic coefficient are presented in the Appendix.

The current distribution and consequently the local state of charge for each cathode particle as a function of location and time for discharge was simulated using Newman's P2D model[32,37] using a control volume method in Python.[38] The simulation parameters for the P2D analysis are summarized in Table I. After obtaining the local state of charge and concentration, the rate of enthalpy change per particle was calculated using Eq. 7. Since P2D assumes that the current seen by all the particles at a distance x (see Fig. 1) from the current collector is the same, the rate of enthalpy change of all the particles within x and $x + dx$ could be assumed to be the same, and the rate of total enthalpy change for all particles in the electrode can be calculated as

$$\sum_{Particles\ per\ unit\ area, Cathode}\left(\frac{dH}{dt}\right) = \frac{3\varepsilon_{ins}}{4\pi R^3}\int_0^{L_{cathode}}\frac{dH}{dt}(x,t)dx \qquad [19]$$

where $\frac{3\varepsilon_{ins}}{4\pi R^3}dx$ is the approximation for the number of particles per unit area between x and $x + dx$.

The set of equations used to quantify the rate of the total enthalpy change and consequently the heat of mixing for a particle and the overall cell (per unit area basis) is summarized in Table II.

Results and Discussion

Taylor expansion approximation and the error associated.— Starting from this fundamental equation of the rate of the total enthalpy change (Eq. 6), Thomas and Newman[7] apply the Taylor expansion approximation (based on the assumption of small concentration gradients within the particles) to obtain the equation:

$$\frac{dH}{dt} = I_p U_{H,\infty} + \frac{d}{dt}\left(\frac{1}{2}\frac{\partial\overline{H_s}}{\partial c_s}\int(c_s - c_{s,\infty})^2 dv\right) \qquad [20]$$

This can be further rearranged into:

$$\frac{dH}{dt} = I_p U_{H,s} + (I_p U_{H,\infty} - I_p U_{H,s}) + \frac{d}{dt}\left(\frac{1}{2}\frac{\partial\overline{H_s}}{\partial c_s}\int(c_s - c_{s,\infty})^2 dv\right) \qquad [21]$$

The first term, evaluated at the surface concentration, is the rate enthalpy change due to the charge transfer reaction at the surface, the second term is generally referred to as enthalpy change due to concentration. The last term $\frac{d}{dt}\left(\frac{1}{2}\frac{\partial\overline{H_s}}{\partial c_s}\int(c_s - c_{s,\infty})^2 dv\right)$, derived by Newman and Thomas (equation number 40 in Thomas and Newman[7]) with the Taylor expansion approximation, is the expression used by various authors ([19–21,27,28]) as "Heat of Mixing."

The Taylor expansion approximation assumes small concentration gradients so that a 2nd order expansion is sufficient to describe the enthalpy difference from the enthalpy evaluated at the mean concentration. At small charge/discharge rates, this assumption is reasonable. However, at higher C-rates, when the rate of lithium influx is significantly greater than the diffusion rate, strong concentration gradients develop, and this approximation is not valid. Shown in Fig. 2 is a comparison of the rate of enthalpy change for the entire cell with a uniform current distribution at 3 different C-rates: 1 C, 5 C and 8 C. As the C-rate increases, the assumption of small concentration gradients does not hold true. At higher C-rates and at certain SOC's where the $\frac{\partial\overline{H_s}}{\partial c_s}$ term is large, the results from the Taylor expansion calculations deviate/overshoot significantly from the actual enthalpy change rate calculated from Eq. 6.

In Fig. 3, we have quantified the maximum error (with respect to the rate of enthalpy change calculated from Eq. 6 and normalized by the range of the enthalpy change rate) as a function of the C-rate in predicting the rate of enthalpy change with the Taylor expansion

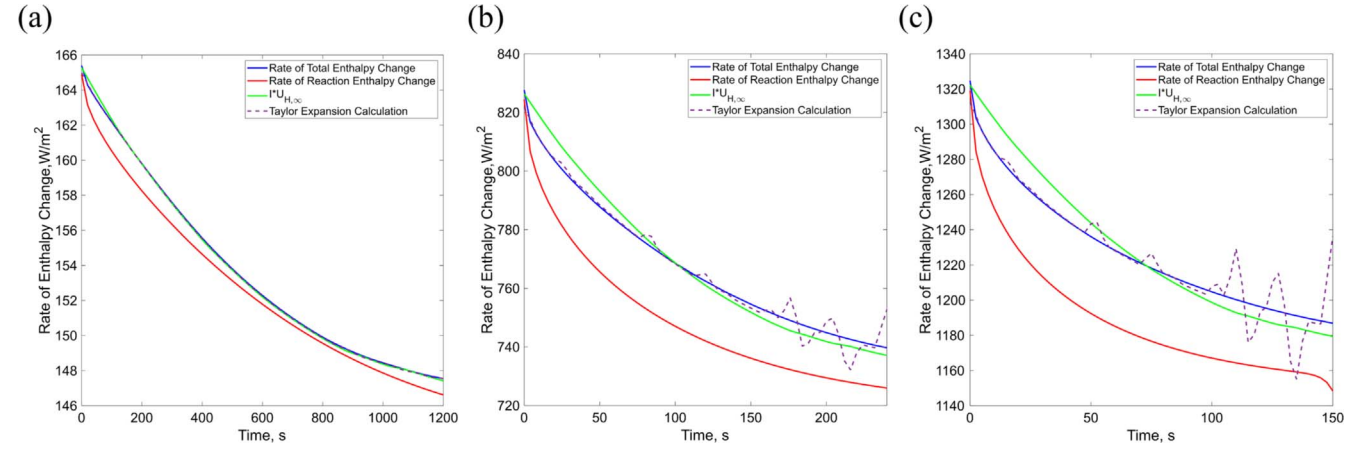

Figure 2. Enthalpy Change simulated from rate of the total enthalpy change calculation and the method of Taylor Expansion for NMC523 for (a) 3 C (b) 6 C and (c) 8 C discharge rates. As the discharge rate increases, the error using the Taylor expansion method increases.

Table II. List of equations used in the rate of enthalpy change and the heat of mixing calculation.

	Equation	Eqn. No.
For a particle:		
Rate of the Total Enthalpy Change (Watts):	$\frac{dH}{dt} = -4\pi F \int_0^R r^2 \left(\frac{dc_s(r,t)}{dt}\right) U_H(y(r,t))dr$	7
Heat of Mixing (Watts):	$\dot{Q}_{mixing,particle} = \left(\frac{dH}{dt}\right) - 4\pi R^2 i U_{H,surface}$	17
For the entire Cell (per unit electrode area basis):		
Rate of the Total Enthalpy Change (W m^{-2}):	$\sum_{Particles\ per\ unit\ area,\ Cathode}\left(\frac{dH}{dt}\right) = \frac{3\varepsilon_{ins}}{4\pi R^3}\int_0^{L_{cathode}} \frac{dH}{dt}(x,t)dx$	19
Total Heat Generated (W m^{-2}):	$\dot{Q}_{cell} = \frac{3\varepsilon_{ins}}{4\pi R^3}\int_0^{L_{cathode}} \frac{dH}{dt}(x,t)dx - IV_{cell}$	13, 19
Heat of Mixing (W m^{-2}):	$\dot{Q}_{mixing,cell} = \frac{3\varepsilon_{ins}}{4\pi R^3}\int_0^{L_{cathode}} \left(\frac{dH}{dt}(x,t) - 4\pi R^2 i U_{H,surface}(x,t)\right)dx$	18, 19

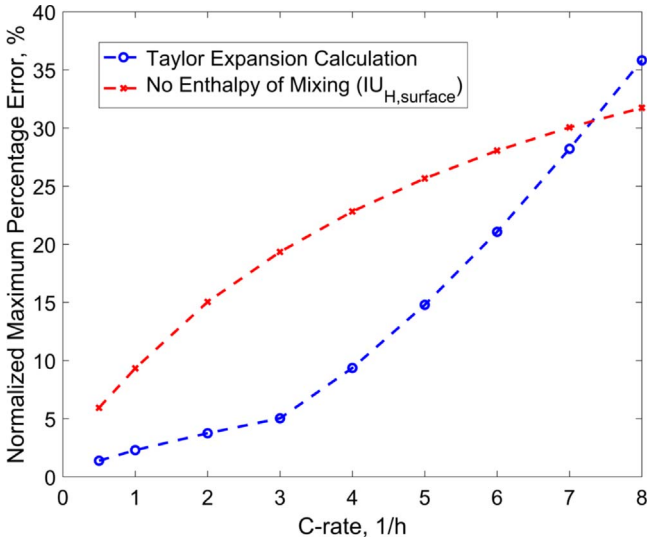

Figure 3. Normalized maximum percentage error associated with calculating the enthalpy change rate with the Taylor expansion approximation as well as not including the enthalpy of mixing at all calculated as a function of C-rate.

method as well as not including heat of mixing at all. As expected, at low C-rates (less than 3 C), the Taylor expansion method incurs low error (<10%), however, as the C-rate goes up, the error increases, to the point that it exceeds the error associated with not including heat of mixing at all (calculating only the rate of enthalpy change due to the reaction). This clearly shows that the Taylor expansion approximation is limited and not applicable during fast charge/discharge, exactly when the heat of mixing becomes important.

Study of the total heat generated and the heat of mixing from the rate of total enthalpy change.—Having established that the method of Taylor expansion is not appropriate for higher C-rates, all subsequent results of the investigation of the total heat generated and the heat of mixing in a cell with NMC523 cathode are calculated from the rate of the total enthalpy change using the method described in section 2 and summarized in Table II. Figures 4a and 4b show the total enthalpy change, reaction enthalpy change and the work done by the cell (IV) for two different charge rates 1 C and 3 C respectively. It can be seen from the figure that at 1 C, the curve for rate of change of reaction enthalpy is very close to the curve of rate of total enthalpy change, However, for 3 C, the two curves differ noticeably. While charging or discharging at a higher C-rate, the net lithium flux in or out of the particle is high compared to the diffusion rate. Because of this, the surface concentration of lithium differs significantly from the concentration of lithium inside the particle,

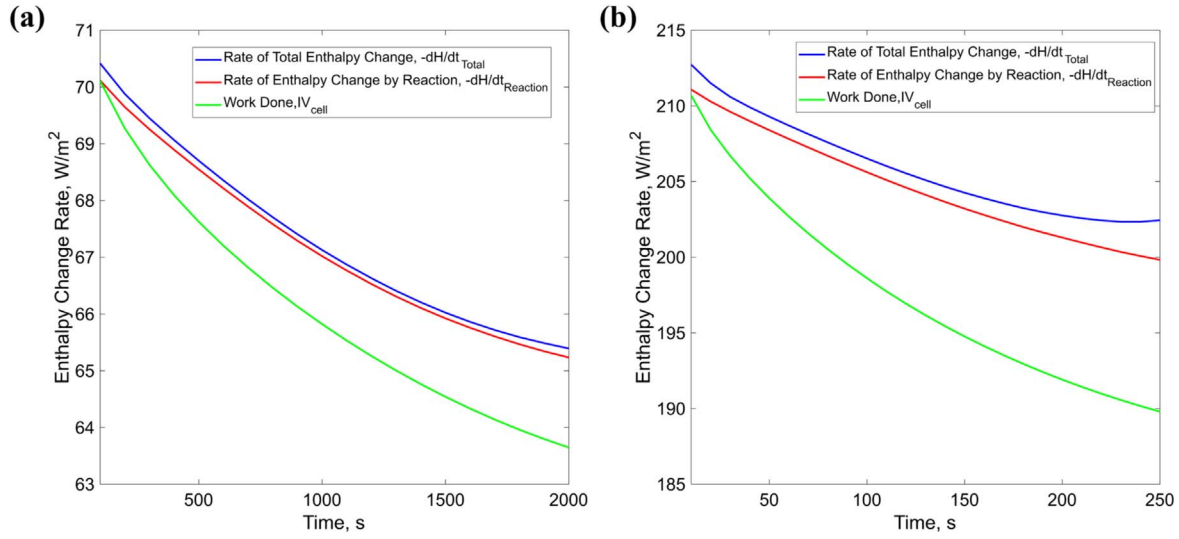

Figure 4. Enthalpy Change during (a) 1 C (b) 3 C discharge. At a lower discharge rate (1 C), almost all of the enthalpy change comes from the reaction. However, at a higher discharge rate (3 C), the overall enthalpy change is significantly greater than the reaction enthalpy change.

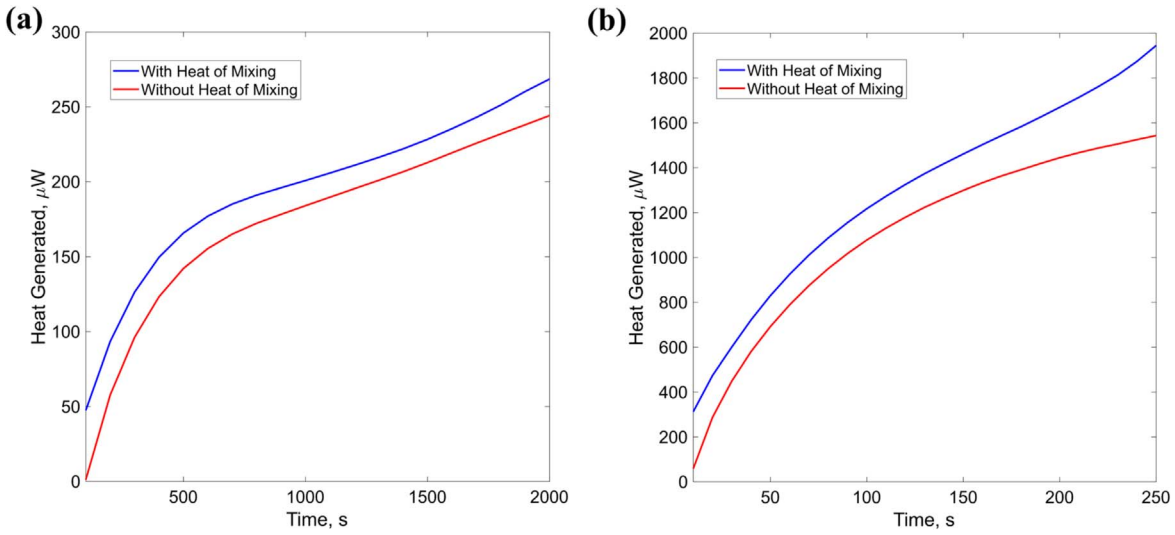

Figure 5. Heat generated during (a) 1 C (b) 3 C discharge. Mixing contributes significantly to the total enthalpy change at a higher C-rate which makes the total heat generated much higher than predicted by including reaction enthalpy alone.

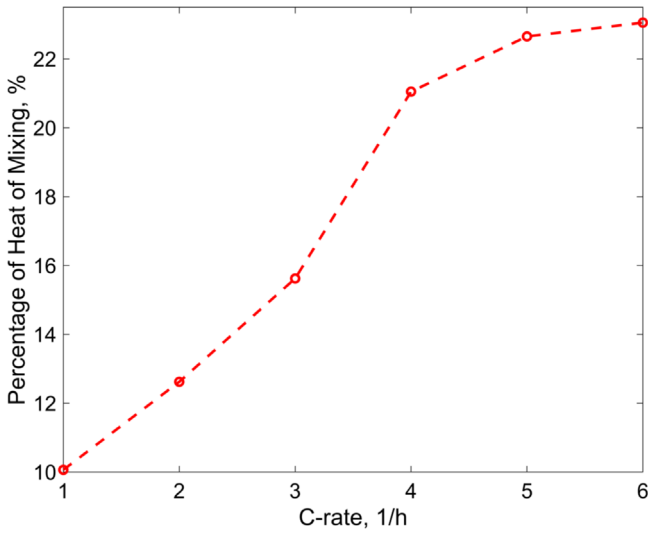

Figure 6. Percentage contribution of heat of mixing in the overall heat generated. Mixing can thus contribute nearly 1/5 of the total heat generated at high C-rates.

and strong concentration gradients develop within the particles. When lithium diffuses through such a gradient in concentration, the local composition and therefore the energy changes rapidly, and as the change in energy is exothermic, it is manifested as heat. At lower C-rates however, the rate of diffusion is comparable to the lithium flux in or out of the particle, because of which strong concentration gradients do not develop. For a lithium atom diffusing inside a particle with weak concentration gradients, the local composition does not change rapidly as it diffuses. Because of this, the rate of change of its enthalpy due to the change in local composition is low compared to the change in enthalpy due to the electron transfer reaction at the surface. This is the precisely why most of the rate of enthalpy change is contributed by the reaction alone for the 1 C discharge, while a significant portion of the total enthalpy change for 3 C discharge is contributed by mixing.

The heat generated is the difference between the enthalpy change and the work done. Figures 5a and 5b show the heat generated calculated with and without including heat of mixing. It can be seen that at a lower C-rate (1 C), the error induced by not including heat of mixing is small when compared to that in the case of a higher C-rate (3 C), which can again be explained by the presence or absence of the concentration gradients.

The time average of percentage of heat of mixing in the overall heat generated was quantified for different C-rates and the result is presented in Fig. 6. It is evident from the figure that even at 1 C, heat of mixing is significant and contributes up to 10% of the total heat generated. At higher C-rates, the heat of mixing contribution further increases, where at 6 C it can be up to 23%. This is a major observation because most heat generation models in literature had been neglecting heat of mixing considering it as insignificant, and those models that did include it had been calculating it incorrectly. This result, however, shows that if calculated correctly, the heat of mixing can be a significant source of heat generation and therefore demonstrates a need for revision of literature in order to understand and quantify heat generation accurately.

Finally, it is also worth discussing the irreversible exothermic nature of heat of mixing in Lithium insertion compounds. Unlike entropic (reversible) heat, heat of mixing is exothermic for both charge and discharge. This is a consequence of the fact that in both charge and discharge, lithium inside a particle diffuses from higher lithium concentration to lower lithium concentration. For an NMC particle, the energy of a composition with higher lithium content is higher than that with lower lithium content. Thus, the diffusion process always makes lithium move from a state with a higher energy to a state with a lower energy. Hence, this movement of lithium (mixing) is always exothermic regardless of whether the battery is charging or discharging. This irreversible exothermic nature of heat of mixing arising from diffusion into a state of lower energy is inherently different from irreversible heat arising from reaction overpotential or Ohmic losses which arise from kinetic or transport limitations (losses). Had the mixing process been endothermic, heat of mixing would have been irreversibly endothermic.

Conclusions

From the original papers on battery heat generation,[7,13,16] it is evident that the methods commonly used to calculate the rate of enthalpy change (and consequently the heat generation) such as $IU_{H,surface}$, or $IU_{H,\infty}$ or the method of Taylor expansion are approximations to the fundamental equation of the rate of total enthalpy change (Eq. 6). At lower charge/discharge rates, these approximations work reasonably well. However, at high charge/discharge rates, these approximations do not accurately represent the rate of the enthalpy change as the assumptions made for the approximations are not valid when the concentration gradients are

strong. In that case, calculating the rate of the enthalpy change and the heat of mixing without approximations by reverting to the fundamental equation of the rate of the total enthalpy change becomes necessary. Using the fundamental equation, we have shown in this paper that, in NMC cathodes operating under realistic fast charge/discharge conditions, the heat of mixing contributes to a significant portion of the heat generated (nearly 1/5 at 6 C) and therefore should not be neglected from modeling. Additionally, we have also established when and how the Taylor expansion approximation for calculating the heat of mixing breaks down and quantified the error associated with it. In the process, we have also clarified the meaning of heat of mixing and discussed its irreversible exothermic nature in Li-ion batteries with NMC cathodes.

Acknowledgments

This work was supported by the Assistant Secretary for Energy Efficiency and Renewable Energy, Vehicles Technology Office, of the U.S. Department of Energy under Contract No. DEAC02-05CH11231.

Appendix

Calorimetry Data, Open Circuit Potential and Entropic Coefficient for NMC523:

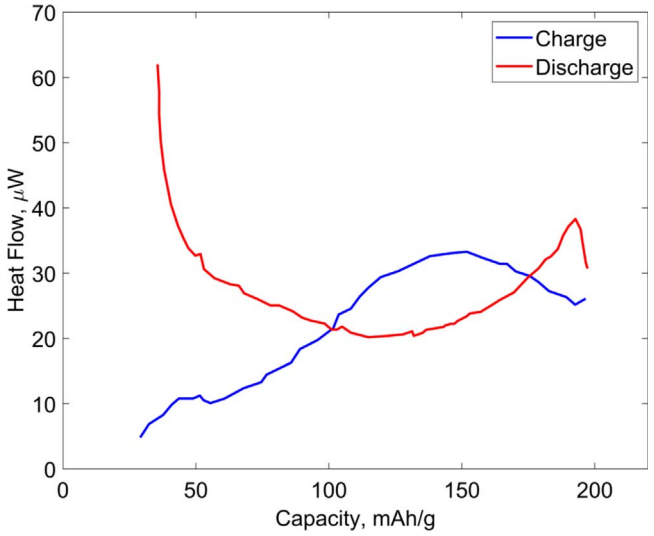

Figure A·1. Calorimetry data used to calculate the entropic coefficient. Both charge and discharge are carried out at C/10.

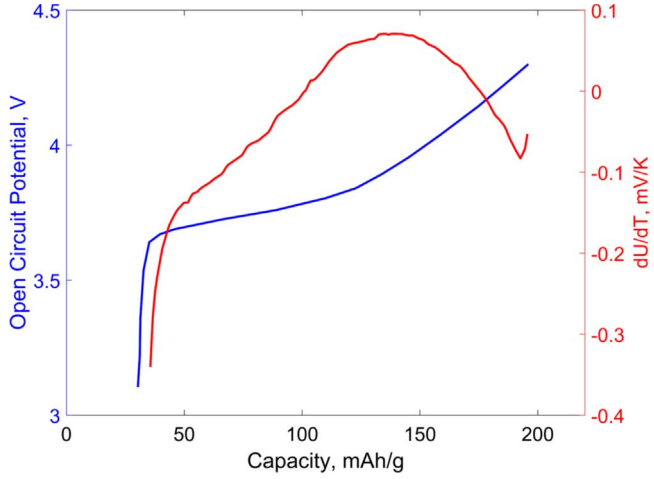

Figure A·2. Open Circuit Potential (Blue) and Entropic Coefficient (Red) for NMC523.

ORCID

Divya Chalise https://orcid.org/0000-0001-6197-355X
Ravi Prasher https://orcid.org/0000-0002-3282-7147

References

1. Y. Liu, Y. Zhu, and Y. Cui, "Challenges and opportunities towards fast-charging battery materials." *Nat. Energy*, **4**, 540 (2019).
2. M. Keyser et al., "Enabling fast charging – battery thermal considerations." *J. Power Sources*, **367**, 228 (2017).
3. D. Chalise, K. Shah, R. Prasher, and A. Jain, "Conjugate heat transfer analysis of air/liquid cooling of a Li-ion battery pack." *J. Electrochem. Energy Convers. Storage.*, **15**, 1 (2017).
4. T. Waldmann, M. Wilka, M. Kasper, M. Fleischhammer, and M. Wohlfahrt-Mehrens, "Temperature dependent ageing mechanisms in Lithium-ion batteries - a post-mortem study." *J. Power Sources*, **262**, 129 (2014).
5. T. M. Bandhauer, S. Garimella, and T. F. Fuller, "A critical review of thermal issues in lithium-ion batteries." *J. Electrochem. Soc.*, **158**, R1 (2011).
6. X. Feng, M. Ouyang, X. Liu, L. Lu, Y. Xia, and X. He, "Thermal runaway mechanism of lithium ion battery for electric vehicles: a review." *Energy Storage Mater.*, **10**, 246 (2018).
7. K. E. Thomas and J. Newman, "Thermal modeling of porous insertion electrodes." *J. Electrochem. Soc.*, **150**, A176 (2003).
8. J. Newman and K. E. Thomas, *Electrochemical Systems* (John Wiley & Sons, Inc, Hoboken, New Jersey) 3rd ed. (2004).
9. K. E. Thomas and J. Newman, "Heats of mixing and of entropy in porous insertion electrodes." *J. Power Sources*, **119–121**, 844 (2003).
10. T. Bandhauer, S. Garimella, and T. F. Fuller, "Electrochemical-thermal modeling to evaluate battery thermal management strategies: II. Edge and internal cooling." *J. Electrochem. Soc.*, **162**, A137 (2014).
11. S. J. Drake, M. Martin, D. A. Wetz, J. K. Ostanek, S. P. Miller, J. M. Heinzel, and A. Jain, "Heat generation rate measurement in a Li-ion cell at large C-rates through temperature and heat flux measurements." *J. Power Sources*, **285**, 266 (2015).
12. S. Du, Y. Lai, L. Ai, L. Ai, Y. Cheng, Y. Tang, and M. Jia, "An investigation of irreversible heat generation in lithium ion batteries based on a thermo-electrochemical coupling method." *Appl. Therm. Eng.*, **121**, 501 (2017).
13. L. Rao and J. Newman, "Heat-generation rate and general energy balance for insertion battery systems." *J. Electrochem. Soc.*, **144**, 2697 (1997).
14. K. E. Thomas, *Lithium-Ion Batteries: Thermal and Interfacial Phenomena* (University of California, Berkeley, California) (2002).
15. C. R. Pals and J. Newman, "Thermal modeling of the lithium/polymer battery I. Discharge behavior of a single cell." *J. Electrochem. Soc.*, **142**, 3274 (1995).
16. D. Bernardi, E. Pawlikowski, and J. Newman, "A general energy balance for battery systems." *J. Electrochem. Soc.*, **132**, 5 (1985).
17. K. An, P. Barai, K. Smith, and P. P. Mukherjee, "Probing the thermal implications in mechanical degradation of lithium-ion battery electrodes." *J. Electrochem. Soc.*, **161**, A1058 (2014).
18. K. Kumaresan, G. Sikha, and R. E. White, "Thermal model for a Li-Ion cell." *J. Electrochem. Soc.*, **155**, A164 (2008).
19. X. Zhang, *Multiscale Modeling of Li-ion Cells: Mechanics, Heat Generation and Electrochemical Kinetics* (University of Michigan, Ann Arbor, Michigan) (2009).
20. B. Yan, C. Lim, L. Yin, and L. Zhu, "Simulation of heat generation in a reconstructed LiCoO2 cathode during galvanostatic discharge." *Electrochim. Acta*, **100**, 171 (2013).
21. M. Farag, H. Sweity, M. Fleckenstein, and S. Habibi, "Combined electrochemical, heat generation, and thermal model for large prismatic lithium-ion batteries in real-time applications." *J. Power Sources*, **360**, 618 (2017).
22. X. Zhang, A. M. Sastry, and W. Shyy, "Intercalation-induced stress and heat generation within single lithium-ion battery cathode particles." *J. Electrochem. Soc.*, **155**, A542 (2008).
23. S. Panchal, M. Mathew, R. Fraser, and M. Fowler, "Electrochemical thermal modeling and experimental measurements of 18650 cylindrical lithium-ion battery during discharge cycle for an EV." *Appl. Therm. Eng.*, **135**, 123 (2018).
24. W. Huo, H. He, and F. Sun, "Electrochemical-thermal modeling for a ternary lithium ion battery during discharging and driving cycle testing." *RSC Adv.*, **5**, 57599 (2015).
25. C. Y. Wang and V. Srinivasan, "Computational battery dynamics (CBD) - electrochemical/thermal coupled modeling and multi-scale modeling." *J. Power Sources*, **110**, 364 (2002).
26. B. Wu, V. Yufit, M. Marinescu, G. J. Offer, R. F. Martinez-Botas, and N. P. Brandon, "Coupled thermal-electrochemical modelling of uneven heat generation in lithium-ion battery packs." *J. Power Sources*, **243**, 544 (2013).
27. Z. Song, *Modeling and Simulation of Heat of Mixing in Li Ion Batteries* (Purdue University, Indianapolis, Indiana) (2015).
28. X. Zhang, A. M. Sastry, and W. Shyy, "Intercalation-induced stress and heat generation within single lithium-ion battery cathode particles." *J. Electrochem. Soc.*, **155**, A542 (2008).
29. S. Schweidler, L. De Biasi, A. Schiele, P. Hartmann, T. Brezesinski, and J. Janek, "Volume changes of graphite anodes revisited: a combined operando X-ray diffraction and in situ pressure analysis study." *J. Phys. Chem. C.*, **122**, 8829 (2018).
30. V. Malavé, J. R. Berger, and P. A. Martin, "Concentration-dependent chemical expansion in lithium-ion battery cathode particles." *J. Appl. Mech. Trans. ASME.*, **81**, 091005-1 (2014).

31. X. Wang, R. Xiao, H. Li, and L. Chen, "Quantitative structure-property relationship study of cathode volume changes in lithium ion batteries using ab-initio and partial least squares analysis." *J. Mater.*, **3**, 178 (2017).
32. T. F. Fuller, M. Doyle, and J. Newman, "Simulation and optimization of the dual lithium ion insertion cell." *J. Electrochem. Soc.*, **141**, 1 (1994).
33. K. Smith and C. Y. Wang, "Power and thermal characterization of a lithium-ion battery pack for hybrid-electric vehicles." *J. Power Sources*, **160**, 662 (2006).
34. W. Lu, H. Yang, and J. Prakash, "Determination of the reversible and irreversible heats of LiNi 0.8Co0.2O2/mesocarbon microbead Li-ion cell reactions using isothermal microcalorimetery." *Electrochim. Acta*, **51**, 1322 (2006).
35. W. Lu, I. Belharouak, J. Liu, and K. Amine, "Thermal properties of Li4/3Ti5/3O4/LiMn2O4 cell." *J. Power Sources*, **174**, 673 (2007).
36. W. Lu, I. Belharouak, S. H. Park, Y. K. Sun, and K. Amine, "Isothermal calorimetry investigation of Li1+xMn2-yAlzO4 spinel." *Electrochim. Acta*, **52**, 5837 (2007).
37. J. Newman and W. Tiedemann, "Porous-electrode theory with battery applications." *AIChE J.*, **21**, 25 (1975).
38. Python 2.7.17 documentation, Python Softw. Found. https://docs.python.org/2/index.html.
39. J. Sturm, A. Rheinfeld, I. Zilberman, F. B. Spingler, S. Kosch, F. Frie, and A. Jossen, "Modeling and simulation of inhomogeneities in a 18650 nickel-rich, silicon-graphite lithium-ion cell during fast charging." *J. Power Sources*, **412**, 204 (2019).
40. T. Nishida, K. Nishikawa, and Y. Fukunaka, "Diffusivity measurement of LiPF6, LiTFSI, LiBF4 in PC." *ECS Trans.*, **6**, 1 (2008).
41. R. Amin and Y. M. Chiang, "Characterization of electronic and ionic transport in Li1-xNi0.33Mn0.33Co0.33O2 (NMC333) and Li1-xNi0.50Mn0.20Co0.30O2 (NMC523) as a function of Li content." *J. Electrochem. Soc.*, **163**, A1512 (2016).